ISSN 1064-2269, Journal of Communications Technology and Electronics, 2015, Vol. 60, No. 6, pp. 543–551. © Pleiades Publishing, Inc., 2015.
Original Russian Text © M.Yu. Medvedik, M.A. Moskaleva, 2015, published in Radiotekhnika i Elektronika, 2015, Vol. 60, No. 6, pp. 582–590.

ELECTRODYNAMICS AND WAVE PROPAGATION

Analysis of the Problem of Electromagnetic Wave Diffraction on Non-Planar Screens of Various Shapes by the Subhierarchic Method

M. Yu. Medvedik and M. A. Moskaleva

Penza State University, ul. Krasnaya 40, Penza, 440026 Russia

e-mail: _medv@mail.ru

Received January 10, 2014

Abstract—The problem of electromagnetic wave diffraction on a perfectly conducting thin bounded non-planar screens is studied. The concept of generalized canonical computational meshes and generalized matrices is introduced. The subhierarchic method is described in detail. Solutions of the spatial problems of diffraction on screens of complex shapes by the subhierarchic method are obtained.

DOI: 10.1134/S106422691505006X

INTRODUCTION

Solving three-dimensional vector problems of diffraction on non-planar screens of complex shape is an urgent problem of electrodynamics. A widely used method for solving such problems is the method of integral equations, in which the problem is reduced to an intergo-differential equation on a screen [1, 2].

The discretization of the problem is reduced to a finite-dimensional system of linear algebraic equations with a dense (filled) matrix with the dimension on the order of 10^5–10^6. An efficient method for solving diffraction problems on figures of complex shapes is the subhierarchic method described in [3, 4]. The basis functions used in the Galerkin method used for solving the integro-differential equation on a screen were introduced in [5, 6]. The questions of the convergence of numerical methods and other aspects of implementation of the algorithms were discussed in [7, 8].

The current paper continues work [9], in which the problem of diffraction of an external electromagnetic field on perfectly conducting thin bounded screens was considered. The results of the current work form the basis for solving more complex problems on a system of screens and dielectric bodies.

The problem is reduced to solving the vector integro-differential equation [1]

$$\mathrm{L}u := (\operatorname{grad}\mathrm{A}(\operatorname{Div}u) + k^2\mathrm{A}u)\big|_\tau = f, \qquad (1)$$

where A is the integral operator

$$\mathrm{A}u = \int_\Omega \frac{\exp(ik|x-y|)}{|x-y|}u(y)ds, \qquad (2)$$

and Div is the tangent divergence on the screen Ω. Here, τ is the tangential vector, u is the surface current density, k is the wavenumber, and the right-hand side of the equation belongs to the space $C^\infty(\bar{\Omega})$ and is defined as follows:

$$f = 4\pi ikE^0_\tau\big|_\Omega. \qquad (3)$$

1. THE GALERKIN METHOD

Let us consider an n-dimensional space $V_n \subset W$. The unknown u will be approximated by elements $u_n \in V_n$. Using the Galerkin method, we find u_n from the system of equations

$$(Lu_n, v) = (f, v) \quad \forall v \in V_n. \qquad (4)$$

These equations determine a finite-dimensional operator $L_n: V_n \to V_n'$, where V_n' is the space antidual to V_n.

For the convergence of the Galerkin method, it is necessary that the basis function satisfy the approximation property. We use the basis functions φ introduced in [5] and represented in Fig. 1. Here, the basis function $\varphi = \varphi_1$ in Π_1, $\varphi = \varphi_2$ in Π_2, and Π_1 and Π_2 are the rectangles ACC_1A_1 and CBB_1C_1, having a common edge CC_1. Further on, $\varphi_1 = \varphi(M_1)$ and $\varphi_2 = \varphi(M_2)$, where $M_1 \in \Pi_1$ and $M_2 \in \Pi_2$. The functions φ_1 and φ_2 are defined as $\varphi_1 = \overrightarrow{P_1M_1}$, $\overrightarrow{P_1M_1} \| \overrightarrow{AC}$, $P_1 \in AA_1$ and $\varphi_2 = \overrightarrow{P_2M_2}$, $\overrightarrow{M_2P_2} \| \overrightarrow{CB}$, $P_2 \in BB_1$.

In the general case, we may expect that the method converges only when the spaces V_n are limitingly dense in W:

$$\inf_{\psi \in V_n} \|\psi - \varphi\| \to 0, \quad n \to \infty \qquad (5)$$

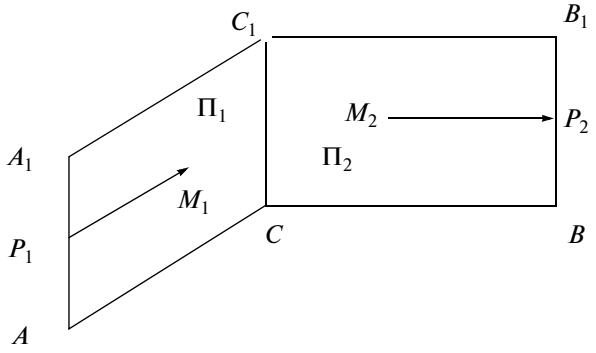

Fig. 1. Basis functions.

for all $\varphi \in X$. This property is called the *approximation property* (an arbitrary element W can be approximated by elements from the subspace V_n with any accuracy in the norm of W).

2. THE GENERALIZED COMPUTATIONAL MESHES AND GENERALIZED MATRICES

For the numerical solution of the problem, we construct a computational mesh Π_N. The discretization of the problem is described in [3, 4]. The use of a definite computational mesh Π_N (whatever fine it is) requires certain restrictions on the geometry of the figure. A particular computational mesh Π_N is constructed for a particular figure G, even of a canonical form. In order to improve the approximation of the boundary ∂G for figures of a complex geometrical shape G, we add additional supports $\mathrm{supp} f_i^k$ for mesh basis functions f_i^k to the computational mesh Π_N, where ith is the order number of the support and k is the type of the support. This makes it possible to apply the subhierarchic method for choosing the mesh basis functions f_i^k. Using additional types of mesh basis functions f_i^k, we can obtain a better approximation of figure's boundary ∂G and minimize the number of basis functions $\mathrm{supp} f_i^k$ in the choice of the geometry vector $\mathbf{W}$. For example, it is hard to approximate a circle by rectangular supports. A circle can be better approximated by triangular supports of mesh basis functions (Fig. 2).

Let us apply the subhierarchic method for choosing the mesh basis functions. To this end, we construct a computational mesh Π_N making it possible to introduce mesh basis functions f_i^k of several different types. Such computational meshes will be called *generalized canonical computational meshes* $\overset{\circ}{\Pi}_N$.

For problems of diffraction on plane screens, we can use the generalized canonical computational mesh $\overset{\circ}{\Pi}_N$ presented in Fig. 3. This computational mesh is the union of triangular and rectangular computational meshes. For example, in the spatial case, the generalized computational mesh $\overset{\circ}{\Pi}_N$ can be understood as a computational mesh formed by the faces of elementary rectangular parallelepipeds (finite elements) obtained by the uniform partition of a rectangular parallelepiped of the canonical form. Each face of the elementary parallelepiped (finite element) is divided by diagonal lines into four triangles.

The matrices composed with the use of the generalized computational mesh $\overset{\circ}{\Pi}_N$ will be called *generalized matrices* $\overset{\circ}{\mathbf{A}}$. The *finite elements of the generalized computational mesh* $\overset{\circ}{\Pi}_N$ are rectangles or triangles parallel to one of the planes of the Cartesian coordinate systems and formed by the horizontal, vertical, or diagonal edges of the computational mesh. The *support of a mesh basis function* $\mathrm{supp} f_i^k$ *for a generalized computational mesh* $\overset{\circ}{\Pi}_N$ consists of two noncoinciding finite elements adjacent to one edge, each oriented along one of the planes of the Cartesian coordinate

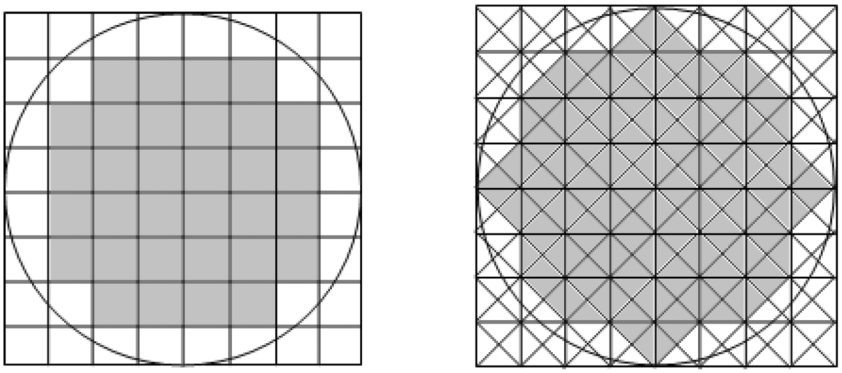

Fig. 2. Approximation of a circular screen.

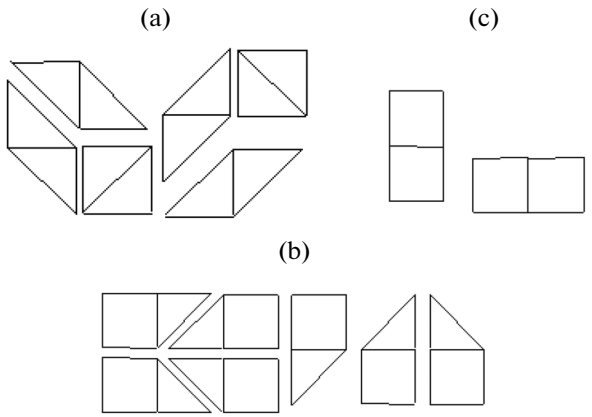

Fig. 3. Templates of the basis functions on a plane.

system. The *template of the supports for a generalized computational mesh* $\overset{o}{\Pi}_N$ is the set of all possible types of supports of the basis functions f_i^k. In the planar case, the generalized computational mesh is a rectangular computational mesh whose each cell is divided into triangles.

In the generalized computational mesh $\overset{o}{\Pi}_N$ presented in Fig. 1, we consider three types of basis functions f_i^k ($k = 1, 2, 3$). The first type ($k = 1$) corresponds to the basis functions f_i^1 constructed on the basis of the template of supports consisting only of triangular finite elements. The second type ($k = 2$) corresponds to the basis functions f_i^2 constructed on the basis of the template of supports consisting only of rectangular finite elements. The third type ($k = 3$) corresponds to hybrid basis functions f_i^3 constructed on the basis of a template containing both rectangular and triangular finite elements. For example, these can be the "rooftop" basis functions, hybrid basis function from [5], or basis function constructed by the Rao–Wilton–Glisson method (RWG) [6].

The templates of the supports for each aforementioned type of basis function are presented in Figs. 3a–3c. The generalized template of supports of the computational mesh presented in Fig. 2 consists of all types of supports.

The use of different types of support for f_i^k makes possible a more convenient approximation of the geometry of various figures. Rectangular figures are more conveniently approximated by rectangular supports; for triangular figures, it is preferable to use hybrid supports of basis functions. More complex geometric figures, e.g., circles, are approximated by triangular supports.

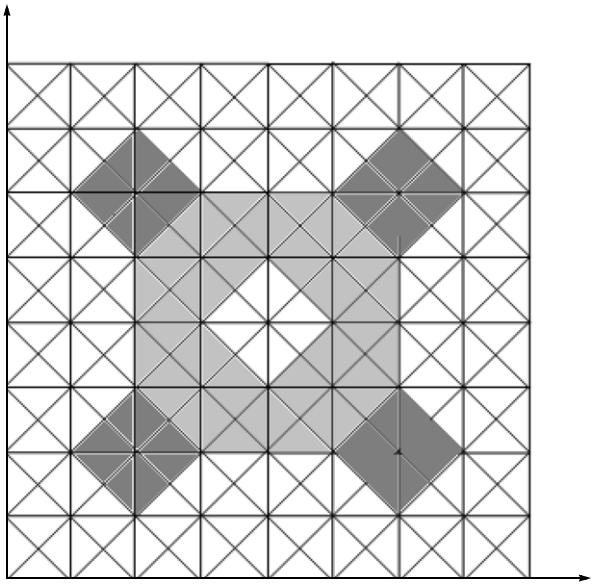

Fig. 4. Generalized canonical computational grid $\overset{o}{\Pi}_N$ on a plane.

Figure 4 shows a generalized computational mesh $\overset{o}{\Pi}_N$ and a figure G of complex shape, constructed on this mesh. In practice, they often use computational meshes $\overset{o}{\Pi}_N$ with supports $\mathrm{supp} f_i^k$ oriented in the same direction (Fig. 5). The algorithm for constructing such meshes is simpler but can encounter problems in the approximation of figure's boundary. On the right of Fig. 5, the figure constructed on the right of Fig. 4 is

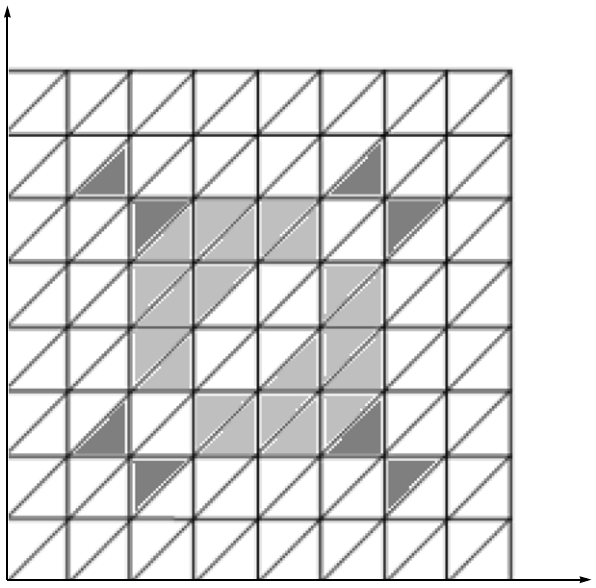

Fig. 5. Approximation with incomplete reconstruction of the figure.

approximated. As we see, the shape of the figure is not reproduced completely but, if we reduce the mesh size, we can specify this figure with a higher accuracy. The following assertion is true.

Any geometrical figure G constructed on a uniform generalized computational mesh $\overset{o}{\Pi}_N$ containing N finite elements along one of the axes can be constructed on a uniform generalized computational mesh $\overset{o}{\Pi}_{2N}$ containing $2N$ finite elements along each of the axes.

Let us consider an arbitrary finite element of the mesh $\overset{o}{\Pi}_N$ containing N finite element along one of the axes. Assume that the finite element considered has a rectangular form. Then, the division of its sides into two equal parts yields four rectangular finite elements completely describing the initial finite element. If the finite element under consideration has a triangular form, this kind of partition of the mesh gives one rectangular finite element and two triangular finite elements, completely describing the initial finite element.

The use of a generalized matrix $\overset{o}{\mathbf{A}}$, makes it possible to efficiently solve the problem of artificial anisotropy arising when the problem is solved on the computational mesh Π_N. The supports of this mesh have a pronounced orientation in one direction (Fig. 5). This leads to an additional error in solving this problem. The generalized computational mesh $\overset{o}{\Pi}_N$ makes it possible to efficiently solve this problem at the stage of specifying the geometry of the figure G due to the possibility of choosing the supports of the basis functions $\mathrm{supp} f_i^k$.

There are different ways of specifying the shape of the figure and its boundary ∂G, using a generalized computational mesh $\overset{o}{\Pi}_N$. The same figure G can be described by several different combinations of the supports of the basis functions, $\sum \mathrm{supp} f_i^k$. It is preferable to use the combinations consisting of the least number of supports. In this case, the problem is solved faster. Another criterion for choosing the supports is the most accurate approximation of figure's boundary. The *uniqueness of specifying the shape* of the figure is guaranteed by the following assertion.

The shape of a figure is specified uniquely if the following two conditions are met:

(1) the edges forming the support do not intersect;

(2) there are no two supports $\mathrm{supp} f_i^k$ formed by one edge and lying in the same plane.

Indeed, the first criterion guarantees that the same support that can be defined by different diagonal edges will not be used twice. The second criterion guarantees that the supports formed by the same edge and lying in the same corresponding planes will not be used simultaneously.

A generalized matrix $\overset{o}{\mathbf{A}}$ consists of matrix elements containing mesh basis functions f_i^k of different types. For solving the problem, it is necessary that each type of mesh basis functions satisfy the approximation condition. Any combination of such basis functions must also satisfy the approximation condition in the chosen spaces. The following assertion is true.

Suppose that a generalized matrix $\overset{o}{\mathbf{A}}$ involves $N \geq 2$ types of basis functions f_i^k ($k = 1, \ldots, N$), each satisfying the approximation condition. Then, any combination of the elements of basis functions of different types satisfying the uniqueness condition will also satisfy the approximation condition.

Indeed, the uniqueness condition guarantees the unique choice of the geometry vector $\mathbf{W}$. Each basis function f_i^k guarantees the approximation within its support, so the set of such basis functions defined on the supports describing a region, guarantees that the approximation condition is satisfied in the entire region.

The size of the generalized matrix $\overset{o}{\mathbf{A}}$ is significantly greater that the size of the matrix constructed for a particular computational mesh. However, the generalized matrix is of the block Toeplitz type. This makes it possible to store only a few rows rather the entire matrix, which substantially simplifies the computations associated with the calculation, storage, and processing of the matrix.

3. APPLICATION OF THE SUBHIERARCHIC METHOD FOR GENERALIZED COMPUTATIONAL MESHES

Applying the projection method to the problem to be solved, we reduce it to a system of linear algebraic equations (SLAE). Using the discretization technique described above, we construct a SLAE in which the matrix and the vector are multi-indexed. Each element of this matrix is obtained by calculating the integral $L_{i,j} = \int_\Omega G(x,y)z(x)\nabla(y)ds$. Here, $x = (x_1, x_2, x_3)$ and $y = (y_1, y_2, y_3)$ are multi-variables, i and j are multi-indices, and $G(x,y)$ is the known Green's function. The right-hand side of the matrix equation describes the behavior of the incident field. The SLAE can be solved by one of the iterative methods.

The subhierarchic method makes it possible to solve problems on figures of a complex geometrical form. Suppose that the figure G consists only of *internal supports* $\Pi_{i_1,\ldots,i_n}$, then, it can be written as follows: $G = \bigcup_i \mathrm{supp}\, f_i$. Here, f_i are the basis functions defined on the support $\mathrm{supp}\, f_i$. Let us specify the geometry of a figure of a complex geometric form, G. To this end, we introduce the geometry vector $\mathbf{W}$ of the length equal to the number of supports that can be con-

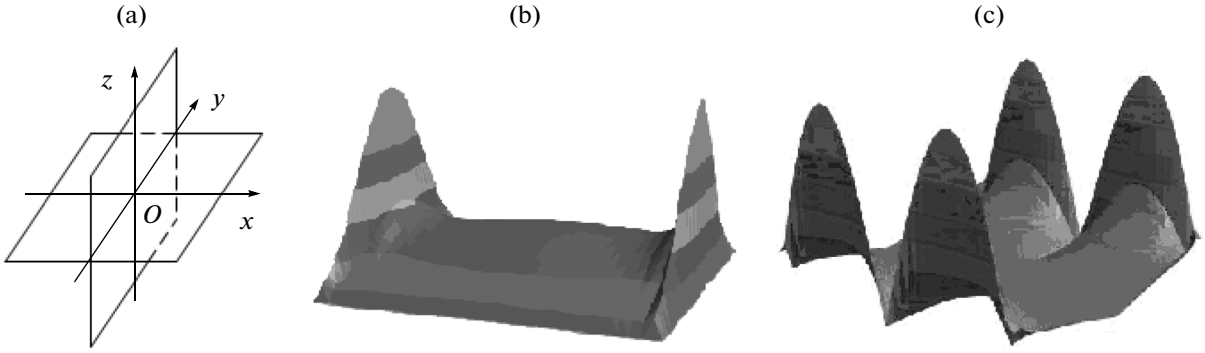

Fig. 6. (a) A plane screen and surface current distribution on it (b) along the x-axis and (c) along the y-axis.

structed on the mesh for a figure of a canonical form. We fill the elements of the vector **W** with zero or unit values: zero, if the template of supports is not defined on the new figure G, and unity, otherwise:

$$\begin{pmatrix} U_{1,\dots,1} \\ U_{1,\dots,2} \\ \dots \\ U_{\dots,q-1,\dots} \\ U_{\dots,q,\dots} \\ U_{\dots,q+1,\dots} \\ \dots \\ U_{n,\dots,n} \end{pmatrix} = \begin{pmatrix} U_{1,\dots,1}W_{1,\dots,1} \\ U_{1,\dots,2}W_{1,\dots,2} \\ \dots \\ U_{\dots,q-1,\dots}W_{\dots,q-1,\dots} \\ U_{\dots,q,\dots}W_{\dots,q,\dots} \\ U_{\dots,q+1,\dots}W_{\dots,q+1,\dots} \\ \dots \\ U_{n,\dots,n}W_{n,\dots,n} \end{pmatrix}, \quad (6)$$

$$W_{\dots,q,\dots} = \begin{cases} 1, & \operatorname{supp} f_{\dots,q,\dots} \in G, \\ 0, & \operatorname{supp} f_{\dots,q,\dots} \notin G. \end{cases}$$

The supports are chosen so that the *uniqueness* condition be satisfied. This procedure will be called the *separation of a figure on a generalized computational mesh*. The separated figure G must be confined inside a canonical figure, i.e., $G \in \Pi$, and be described by a combination of supports.

Let us apply an iterative method to the SLAE obtained by the projection method. The basic operation in the iterative method is the matrix–vector multiplication. Each time, multiplying the matrix **A** by a vector **B**, we will multiply element-wise the obtained vector **U** by the geometry vector **W**.

As a result of solving the SLAE by this method, we will obtain the solution only on the figure of our interest, G.

Suppose that $\overset{\circ}{\mathbf{A}}$ is a generalized matrix obtained by the discretization of integral equation (1) on a figure of a canonical form $\Pi = \{0 < x_1 < d1, \dots, 0 < x_n < dn\}$ by the projection method. Let us introduce the geometry vector **W** and uniquely define the figure of a complex form, G. Applying the subhierarchic method at the stage of solving the SLAE, we will solve the integral equation on the submatrix. The solution found will be the solution of the integral equation on the figure G.

Indeed, by hypothesis, the geometry vector **W** is defined uniquely. This guarantees that the chosen combination of basis functions satisfies the approximation condition. Applying the results of Theorem 1 from [4], we guarantee that the solution found is the solution of the integral equation on the figure G.

By analogy with the vector **W**, we can introduce the vector **V** making it possible to choose the basis functions. This vector can be filled with the numbers 1, 2, …, n, where an arbitrary ith component defines the type of the basis function in the ith support. Transferring the value of the ith component to the basis function, we choose the necessary basis function for the ith support. Introducing the vector of basis functions makes possible a better approximation of figure's boundaries and suppression of artificial anisotropy. The vector of basis functions makes it possible to solve the integral equation on a generalized computational mesh.

4. NUMERICAL RESULTS

Using a subhierarchic method, from a screen of a canonical form, we obtained a rectangular plane screen and non-planar screens of a complex geometrical form, for which the surface currents were calculated.

Below we present the calculation of surface currents on a plane screen. The length of each face was equal to the wavelength λ. The wavenumber k is 2π. The mesh size is 32×32. The incident field had the harmonic form presented in [6]. The directing vector of the incident field is oriented along the y-axis. Figure 6a shows a screen for which the surface current distribution was obtained; Fig. 6b shows the surface current distribution in the plane XOY along the x-axis and Fig. 6c, along the y-axis. The results of solving this problem agree with the solutions obtained by other authors in [5, 6].

In the case of non-planar screens, the numerical calculation of surface currents presented in Figs. 7–13 was performed. The length of each face was equal to

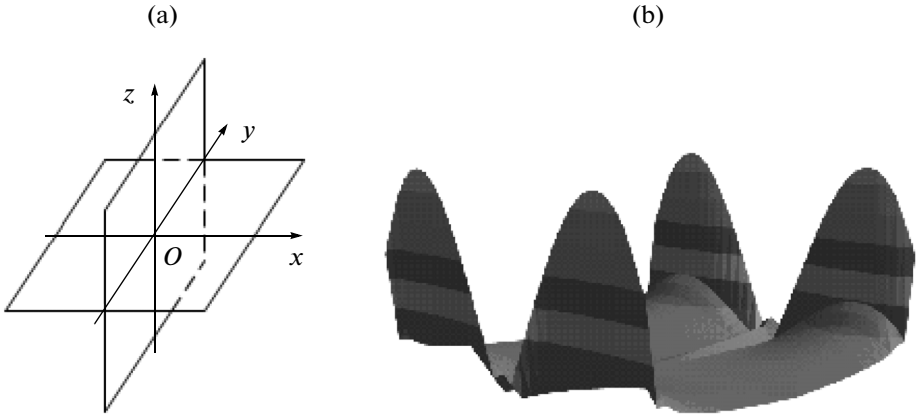

Fig. 7. (a) A cross-shaped screen and (b) surface current distribution on it in the plane *XOY* along the *x*-axis.

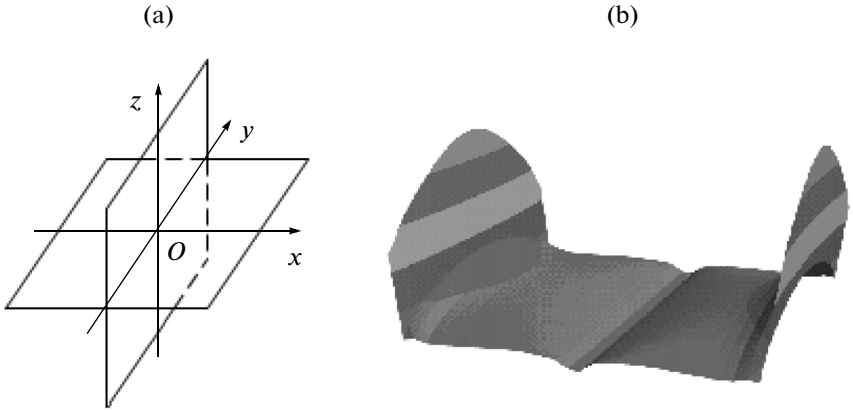

Fig. 8. (a) A cross-shaped screen and (b) surface current distribution on it in the plane *XOY* along the *y*-axis.

the wavelength λ. The wavenumber k was 2π. The grid size was $32 \times 32 \times 32$. The incident field had the harmonic form presented in [6]. The directing vector of the incident field lies in the z-axis. Figures 7a and 8a show a cross-shaped screen, and Figs. 7b and 8b show the surface current distribution on it in the plane *XOY* along the x- and y-axes, respectively.

Figures 9a and 10a also show a cross-shaped screen, and Figs. 9b and 10b show the surface current distribution on it in the plane *YOZ* along the y- and z-axes, respectively. Due to the symmetry of the figure, the results in Fig. 7 and 10 are in a good agreement with one another. The same is true for Figs. 8 and 9.

Figures 11a and 12a also show a screen of a complex geometrical form, and Figs. 11b and 12b show the surface current distribution on it in the plane *XOY* along the x- and y-axes, respectively.

Figures 13a and 14a also show a screen of a complex geometrical form, and Figs. 13b and 14b show the surface current distribution on it in the plane *YOZ* along the y- and z-axes, respectively.

In addition, the surface current distribution on a screen of a complex geometric form was calculated without regard for the corner elements. The results obtained in this case differ from the results presented above in the vicinity of the edge.

It should be noted that the results obtained for a plane screen fully agree with the results presented in [3, 4, 7]. In [8], the convergence of the Galerkin method for the RWG basis functions was proven.

The current distribution on a non-planar screen (on a corner) was described in [9].

From the results of computations, we see that the normal components of the field vanish and the tangential components have a singularity, which agrees with theoretical results.

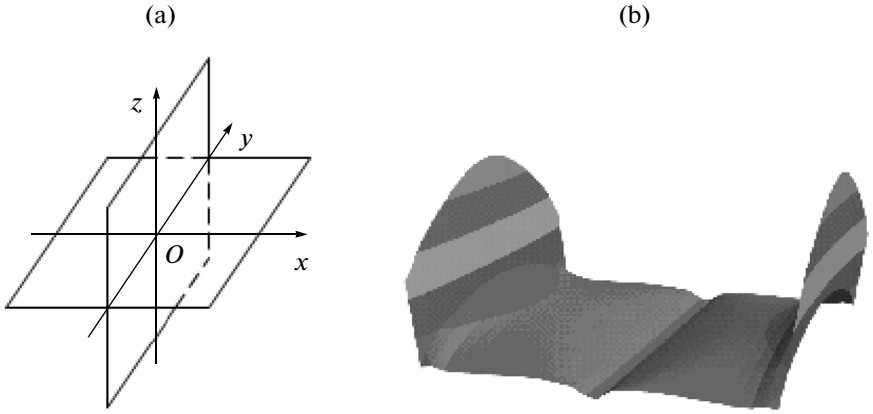

Fig. 9. (a) A cross-shaped screen and (b) surface current distribution on it in the plane *YOZ* along the *y*-axis.

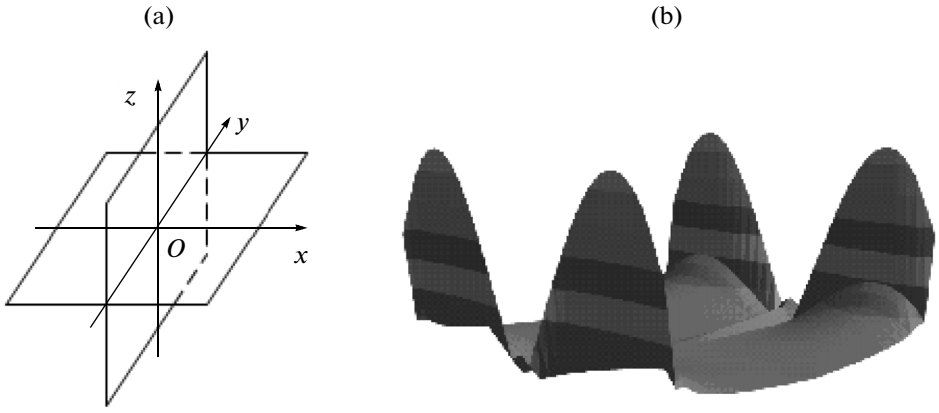

Fig. 10. (a) A cross-shaped screen and (b) surface current distribution on it in the plane *YOZ* along the *z*-axis.

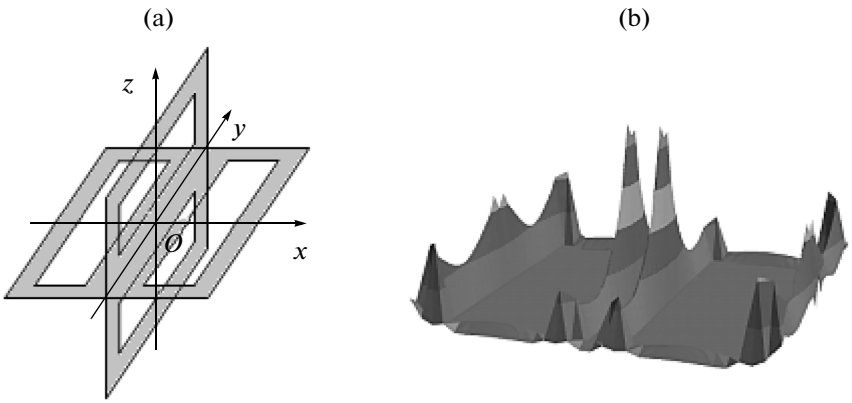

Fig. 11. (a) A screen of complex form and (b) surface current distribution on it in the plane *XOY* along the *x*-axis.

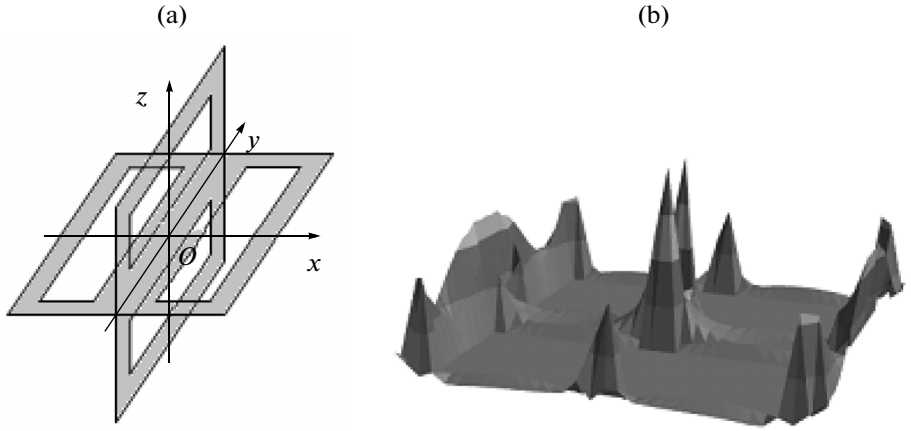

Fig. 12. (a) A screen of complex form and (b) surface current distribution on it in the plane *XOY* along the *y*-axis.

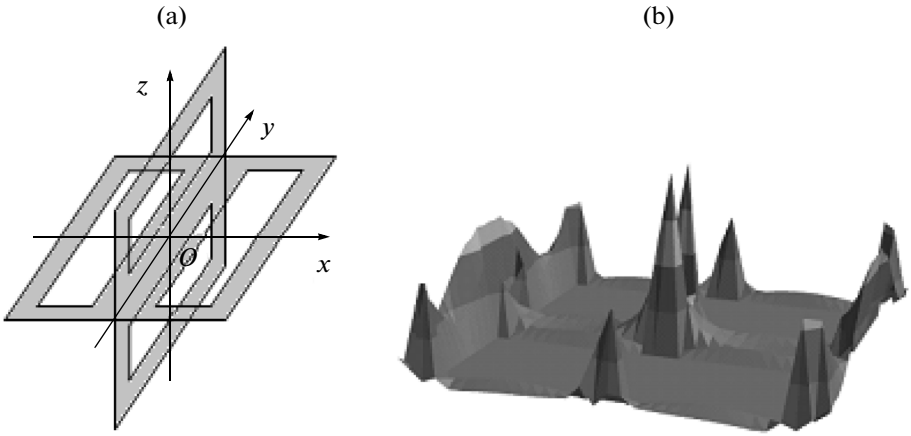

Fig. 13. (a) A screen of complex form and (b) surface current distribution on it in the plane *YOZ* along the *y*-axis.

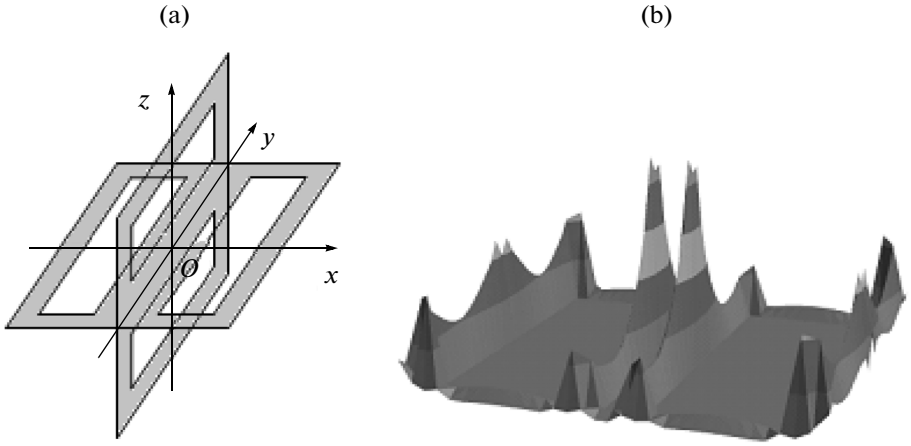

Fig. 14. (a) A screen of complex form and (b) surface current distribution on it in the plane *YOZ* along the *z*-axis.

The calculations were performed on the computer cluster of the Penza State University.

ACKNOWLEDGMENTS

This work was supported by the Russian Scientific Foundation, project no. 14-11-00344.

REFERENCES

1. A. S. Ilinsky and Yu. G. Smirnov, *Electromagnetic Wave Diffraction by Conducting Screens* (Radiotekhnika, Moscow, 1996; VSP, Utrecht, 1998).
2. A. Buffa and S. H. Christiansen, Numerische Mathematik **94** (2), 229 (2003).
3. Yu. G. Smirnov, M. Yu. Medvedik, and M. A. Maksimova, Izv. Vyssh. Uchebn. Zaved., Povolzhskii Region. Fiz. Mat. Nauki, No. 4, 59 (2012).
4. M. Yu. Medvedik, Vychisl. Metody Program. **13** (1), 87 (2012).
5. I. Hänninen, M. Taskinen, and J. Sarvas, Prog. Electromagn. Res., No. 63, 243 (2006).
6. S. M. Rao, D. R. Wilton, and A. W. Glisson, IEEE Trans. Antennas Propag. **30**, 409 (1982).
7. M. Yu. Medvedik, Comput. Math. Math. Phys. **53**, 469 (2013).
8. M. Yu. Medvedik and Yu. G. Smirnov, Comput. Math. Math. Phys. **54**, 114 (2014).
9. M. Yu. Medvedik, J. Commun. Technol. Electron. **58**, 1019 (2013).

Translated by E. Chernokozhin